Available online at www.sciencedirect.com
SCIENCE DIRECT®
Thin Solid Films 494 (2006) 133 – 140
thin solid films
www.elsevier.com/locate/tsf

Adherent diamond coatings on cemented tungsten carbide substrates with new Fe/Ni/Co binder phase

Riccardo Polini [a,*], Michele Delogu [b], Giancarlo Marcheselli [b]

[a] Dipartimento di Scienze e Tecnologie Chimiche, Università di Roma Tor Vergata, Via della Ricerca Scientifica, 00133 Roma, Italy
[b] Fabbrica Italiana Leghe Metalliche Sinterizzate (FILMS) SpA, Via Megolo 2, 28877 Anzola D'Ossola, VB, Italy

Available online 3 October 2005

Abstract

WC–Co hard metals continue to gain importance for cutting, mining and chipless forming tools. Cobalt metal currently dominates the market as a binder because of its unique properties. However, the use of cobalt as a binder has several drawbacks related to its hexagonal close-packed structure and market price fluctuations. These issues pushed the development of pre-alloyed binder powders which contain less than 40 wt.% cobalt. In this paper we first report the results of extensive investigations of WC–Fe/Ni/Co hard metal sintering, surface pretreating and deposition of adherent diamond films by using an industrial hot filament chemical vapour deposition (HFCVD) reactor. In particular, CVD diamond was deposited onto WC–Fe/Ni/Co grades which exhibited the best mechanical properties. Prior to deposition, the substrates were submitted to surface roughening by Murakami's etching and to surface binder removal by aqua regia. The adhesion was evaluated by Rockwell indentation tests (20, 40, 60 and 100 kg) conducted with a Brale indenter and compared to the adhesion of diamond films grown onto Co-cemented tungsten carbide substrates, which were submitted to similar etching pretreatments and identical deposition conditions. The results showed that diamond films on medium-grained WC–6 wt.% Fe/Ni/Co substrates exhibited good adhesion levels, comparable to those obtained for HFCVD diamond on Co-cemented carbides with similar microstructure.

Keywords: Adhesion; Cemented carbides; Chemical vapor deposition (CVD); Diamond

1. Introduction

The interest in superhard (>40 GPa) coating materials has increased significantly during the past 15 years [1]. Diamond is the hardest known material, with a hardness of 70–100 GPa depending on crystallographic orientation and purity, and it exhibits a low friction coefficient and a high thermal conductivity [2]. The synthesis of polycrystalline diamond films by chemical vapor deposition (CVD) has opened up new opportunities to use synthetic diamond in new and innovative applications. In fact, the combination of high hardness and low friction coefficient are key parameters for protective coatings used for wear reduction.

The most suitable substrate material for producing diamond-coated components is Co-cemented tungsten carbide (WC–Co). In fact, the direct deposition of CVD diamond onto WC–Co parts and cutting tools results in components that have extremely high resistance to abrasion while retaining the high fracture toughness of the underlying cemented carbide substrate. As a consequence, diamond coatings on cemented tungsten carbide substrates are increasingly used in engineering applications which have to withstand progressively more arduous conditions [3–10].

WC–Co hard metals continue to gain importance for cutting, mining and chipless forming tools, as well as for high-performance construction and wear parts. Cobalt metal currently dominates the market as a binder because of its unique properties [11]. However, there are also detrimental properties of this binder metal due to its hexagonal close-packed structure [12]. Moreover, the price of cobalt has been relatively unstable during the last years [13]. This was a major incentive in the development of pre-alloyed binder powders which contains less than 40% cobalt and, consequently, are less sensitive to cobalt price fluctuations. Besides the cost-effective nature of pre-alloyed binders, other benefits have emerged. For example, in certain applications, there are positive technical advantages. Prakash made the first inves-

* Corresponding author. Tel.: +39 06 7259 4414; fax: +39 06 7259 4328.
E-mail address: polini@uniroma2.it (R. Polini).

0040-6090/$ - see front matter © 2005 Elsevier B.V. All rights reserved.
doi:10.1016/j.tsf.2005.08.217

tigations on (Fe/Ni/Co)-alloys and showed that cemented tungsten carbides with Fe-rich binders had improved properties such as higher hardness, abrasive wear resistance, toughness and strength compared to Co-bonded hard metals [14]. Moreover, WC–Fe/Ni/Co hard metals show a better oxidation resistance than comparable WC–Co cermets [15] and could contribute to overcome the environmental toxicity of cobalt.

The performance of CVD diamond-coated hard metal components is strongly dependent on the adhesion level of the film. The presence of Co, as well as of other transition metals with a partially filled 3d shell, tends to stabilize sp^2 bonding and to catalyze the formation of amorphous carbon at the diamond/substrate interface [16–18]. The presence of interfacial sp^2-carbon induces the detachment of the diamond deposit from the underlying substrate during use [19–22]. As a result, in the case of diamond-coated articles, it is mandatory to optimize the film adhesion by suitable substrate pretreatments prior to CVD [23–25].

Due to the worldwide increasing interest for both superhard diamond coatings deposited on cemented tungsten carbides and the use of innovative binders for hard metals, in this paper, we report the results of our investigations of WC–Fe/Ni/Co hard metal sintering, surface pretreating and deposition of adherent diamond films by hot filament CVD (HFCVD).

2. Experimental

2.1. Substrate preparation

The substrates used in this work were various kinds of liquid phase sintered hard metals with WC grain sizes of 0.8, 2 and 5 μm and binder contents of 5.8 and 9 wt.%.

For the preparation of fine-grained hard metals, we used a 0.8-μm WC powder (DS80S by H. C. Starck GmbH) doped with 0.27 wt.% VC acting as grain growth inhibitor. For medium- and coarse-grained cemented tungsten carbides, we used ET 5300 and ET 5722 tungsten carbide powders supplied by Eurotungstene®, whose average particle size is 2 μm and 5 μm, respectively. The metallic binders we employed were either a pre-alloyed Fe/Ni/Co powder (30/30/40 supplied by H.C. Starck GmbH), whose physical and chemical parameters are reported in Table 1 or pure Co powder (OMG Kokkola Chemicals Oy).

The metallic binder and tungsten carbide powders were wet-mixed in isopropyl alcohol containing 2% organic binder referred to the total mass of each charge and ball-milled for 72 h. The dried cakes were crushed and sieved to 20 mesh granules. They were formed into rectangular bars in a hard die at 1 ton/cm^2 using a Dorst TPA-12 press.

Table 1
Physical and chemical parameters of pre-alloyed Fe/Ni/Co metal powder used as a binder for hard metals

% Fe	30.22
% Ni	29.88
% Co	39.70
% O	0.640
% C	0.002
Specific surface area (BET, m^2/g)	2.16
Average particle size (μm)[a]	0.85

[a] Measured with a Fisher Sub-Sieve sizer.

Prior to sintering, the green bars were submitted to a two-step thermal treatment (3 h at 450 °C + 1 h at 700 °C) in an atmosphere containing 75 vol.% H_2 and 25 mol.% N_2. Then the samples were submitted to a 1-h sinter-HIP (a process combining sintering and hot isostatic pressing into a single operation) at 1400, 1460 or 1500 °C in argon (3.5 MPa).

The density of the sintered cemented carbides was measured by immersion. Hardness of the materials was determined according to Vickers (HV10) and Rockwell A (HRA) at room temperature. Transverse rupture strength (TRS) measurements were carried out as three-point bending tests according to ISO 3327 in order to provide an indication of toughness of the sintered materials and to compare the TRS values of hard metals sintered with innovative binder (Fe/Ni/Co) to the strength of Co-cemented tungsten carbides having the same WC grain size and binder content. Magnetic saturation and coercivity were measured with a Foerster Koerzimat model CS 1.096 instrument. Mirror-polished samples were characterized by field emission scanning electron microscopy (FE-SEM, Leo Supra 35), energy-dispersive spectroscopy (EDS, Oxford Inca 300) and X-ray diffraction (XRD, Philips X'Pert Pro, graphite filtered Cu Kα radiation).

In Table 2, the chemical compositions and properties of all sintered materials are summarized.

Prior to diamond deposition, the substrates were submitted to a two-step chemical treatment. A first etching step using Murakami's reagent (10 g $K_3[Fe(CN)_6]$ + 10 g KOH + 100 ml water) was carried out at room temperature for 12 min in an ultrasonic bath to etch the WC phase of the cemented carbide, followed by a rinse with distilled water. The second etching step was performed using either a solution of HNO_3/H_2O = 1:1, or Caro's acid (3 ml 96 wt.% H_2SO_4 + 88 ml 30% w/v H_2O_2) or aqua regia (royal water; three parts by volume of concentrated HCl and one part of concentrated HNO_3) at 30 °C.

The duration of the second etching step was varied between 5 and 600 s in order to evaluate the time evolution of the binder concentration detectable by EDS at the substrate surface.

2.2. CVD diamond deposition

Diamond films were deposited onto 10 × 10 × 3-mm substrates using a hot filament chemical vapour deposition (HFCVD) industrial reactor developed by FILMS SpA in collaboration with the Department of Chemical Sciences and Technologies of the University of Rome Tor Vergata. The substrates were placed at 12 mm from an array of horizontal tungsten filaments, which measured 0.76 mm in diameter and 140 mm in length. The gas phase was a mixture of methane and hydrogen containing 2.0% (v/v) CH_4 with an excess of H_2. The total flow rate was 2000 standard cm^3/min and the pressure during deposition was 3 kPa. Deposition temperature was controlled by Type K thermocouples and maintained at 750 ± 30 °C. During the whole deposition process, the filament

Table 2
Composition, sintering parameters and properties of hard metals

Hard metal	WC grain size [μm]	Binder		Sintering T [°C]	Density [g/cm^3]	HV10	HRA	TRS [MPa]	Coercivity [Oe]	Magnetic saturation [Gauss cm^3 g^{-1}]
		Composition	Wt.%							
B-33A	~0.8	Fe/Ni/Co	5.8	1400	14.365	1614	92.2	967	288	70
B-33B	~0.8	Fe/Ni/Co	5.8	1460	14.640	1750	93.2	883	276	91
B-33C	~0.8	Fe/Ni/Co	5.8	1500	14.746	1796	93.3	1165	302	109
B-30	~0.8	Co	5.8	1500	14.816	1743	93.3	3605	333	140
B-37	~0.8	Fe/Ni/Co	9	1500	14.448	1566	92.1	2597	220	143
B-24	~0.8	Co	9	1500	14.484	1551	92.3	3492	247	144
H-10A	2	Fe/Ni/Co	5.8	1400	14.906	1357	90.3	2689	75	145
H-10B	2	Fe/Ni/Co	5.8	1460	14.897	1386	90.3	2822	76	152
H-10C	2	Fe/Ni/Co	5.8	1500	14.897	1338	89.9	2869	72	153
H-4	2	Co	5.8	1500	14.949	1521	91.7	3498	162	136
H-15A	2	Fe/Ni/Co	9	1400	14.538	1245	89.2	2760	67	148
H-15B	2	Fe/Ni/Co	9	1460	14.511	1219	89.0	2581	69	148
H-15C	2	Fe/Ni/Co	9	1500	14.513	1231	88.7	2769	68	151
H-13	2	Co	9	1500	14.615	1275	90.3	3468	119	137
X-6	5	Fe/Ni/Co	5.8	1500	14.841	1289	89.5	1326	59	134
X-4	5	Co	5.8	1500	14.948	1338	90.0	2926	133	129
X-10	5	Fe/Ni/Co	9	1500	14.527	1061	86.9	2587	34	144
X-7	5	Co	9	1500	14.604	1250	89.0	3391	125	143

temperature was in the 2200–2300 °C range, as monitored by a two-colour pyrometer. The deposition time was 22 h, thus ensuring a diamond film thickness of 20–24 μm. The morphology of the diamond coatings was assessed by SEM.

Raman spectroscopy measurements were performed in back-scattering geometry at room temperature by using a Dilor XY triple spectrometer equipped with a liquid nitrogen-cooled charge-coupled device (CCD) detector and an adapted Olympus microscope. The spectra were excited with an Ar^+ laser (514.5 nm). The lines of a neon lamp were used for frequency-scale calibration. The scattered light was not analyzed in polarization. The spectral resolution was 0.5 cm^{-1}.

2.3. Adhesion tests

In order to evaluate the adhesion level of the diamond coatings, we performed indentation tests using a Volpert Rockwell hardness tester with a conical diamond indenter (120° cone angle and 0.2 mm tip radius) [26]. Each deposited sample was tested by applying loads of 20, 40, 60 and 100 kg at the diamond indenter. The larger the load value which provoked the film delamination, the better the adhesion. The indenter was replaced with a new one after one set of measurements. The substitution of a new indenter was necessary because of the modification of the tip geometry, which was controlled by performing Rockwell A (HRA, 60 kg) hardness measurements on a standard cemented carbide sample with certified hardness.

3. Results and discussion

3.1. Microstructure and mechanical properties of Fe/Ni/Co-cemented carbides

Fig. 1 shows the microstructure of six hard metals sintered at 1500 °C using Fe/Ni/Co as a binder. The micrograph of sample B-33C illustrates that the fine-grained material sintered with 5.8 wt.% Fe/Ni/Co exhibited a visible residual porosity, which was responsible for the low TRS value (1165 MPa). Although the data in Table 2 show that, in the case of B-33 hard metals, an increase in sintering temperature led to larger densities and better mechanical properties, however, the density of B-33C sample was lower than both the H-10C and X-6 carbides having the same Fe/Ni/Co content and sintered at the same temperature. This fact confirmed that the preparation of dense and tough hard metals using both fine-grained WC and 5.8 wt.% Fe/Ni/Co is still a challenge for hard metal manufacturers. The B-37 sample showed a slightly lower density value (14.448 g/cm^3) than both the H-15C and X-10 cemented carbides, whose densities were 14.513 and 14.527 g/cm^3, respectively. Therefore, as confirmed by SEM micrographs in Fig. 1, the larger amount of binder phase (9 wt.%) allowed us to reduce the residual porosity of fine-grained sintered samples and to obtain an acceptable TRS value, which was larger than 2500 MPa and 26% lower than the TRS value of the corresponding Co-cemented tungsten carbide (B-24).

The microstructure of medium-grained hard metals (H-10 and H-15) was much more homogeneous, with very low porosity. These cemented carbides exhibited higher density values with respect to the other Fe/Ni/Co-cemented carbides having the same binder content (Table 2). Their densities were practically independent of the sintering temperature, and this fact indicates the good sinterability of medium-grained hard metals produced using Fe/Ni/Co as a binder. Moreover, their transverse rupture strength and hardness values were slightly smaller than TRS and HRA values of the corresponding Co-cemented tungsten carbides (H-4 and H-13 hard metals), thus indicating an adequate mix of mechanical properties.

The micrograph of Fe/Ni/Co-cemented carbides prepared using the coarser WC powder showed that the microstructure

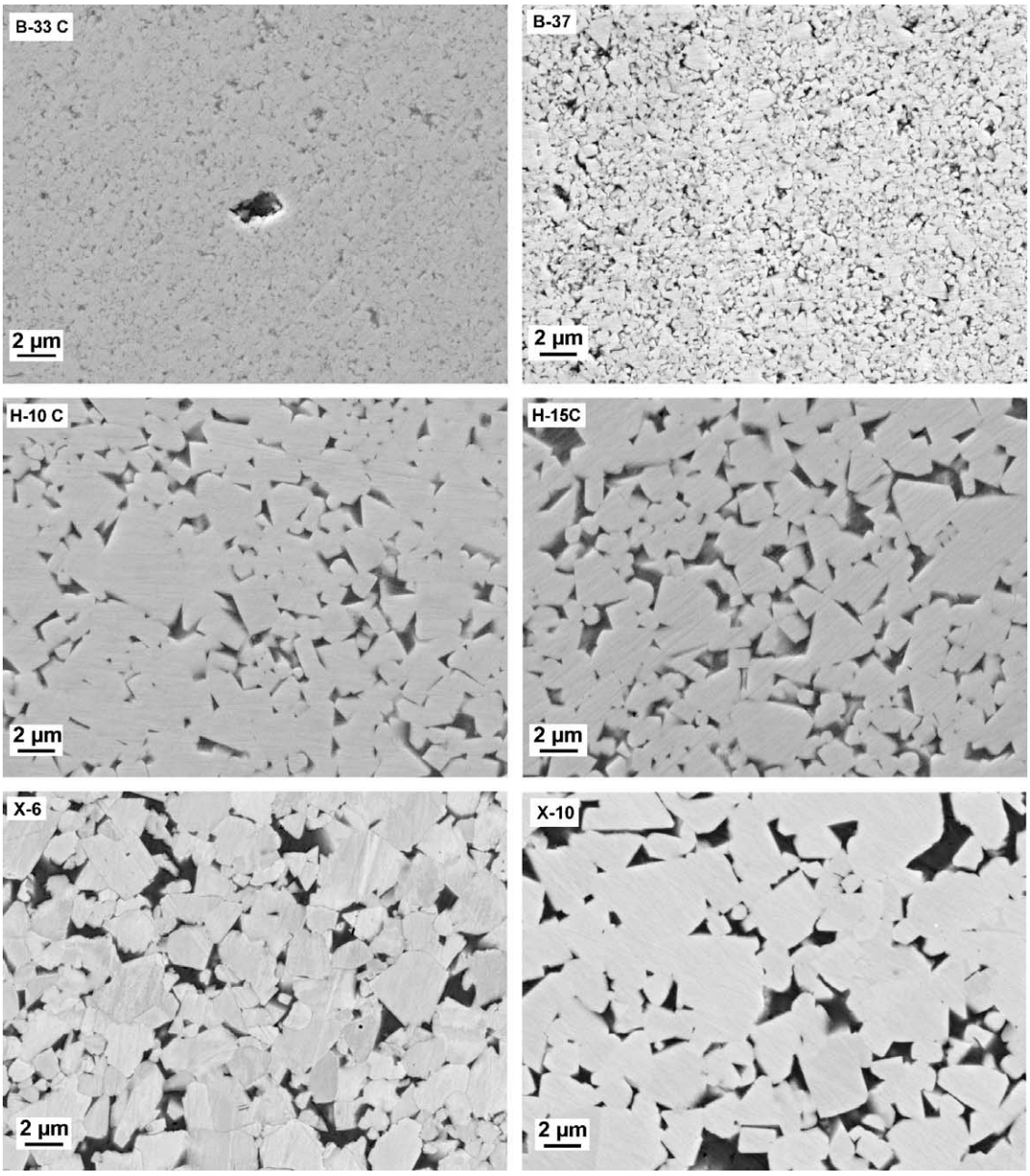

Fig. 1. SEM micrographs showing the microstructure of Fe/Ni/Co-cemented tungsten carbides with different grain size and 5.8 wt.% (left column) or 9 wt.% (right column) binder content (Table 2).

of the hard metal containing the lower (5.8 wt.%) binder content (X-6) was characterized by smaller grains than the ones detected for the X-10 sample. This fact has to be ascribed to the presence of η-phase (revealed by XRD, as discussed below) and to the fragmentation of larger particles during ball-milling when the coarse WC powder was mixed with 5.8 wt.% binder, and to the oversintering of WC grains in the X-10 sample, which was favoured by the larger amount of liquid binder phase. These data indicate that the sintering of coarse-grained hard metals using pre-alloyed Fe/Ni/Co powders still remains a difficult task.

Fig. 2 shows the XRD patterns of WC–5.8 wt.% Fe/Ni/Co hard metals sintered at 1500 °C. The data revealed the occurrence of mixed carbides only in the case of X-6 hard metal. In fact, the formation of a Me_3W_3C (η_{33}, with Me=Fe, Ni or Co) phase was confirmed by the weak reflection at 42.18°, in good agreement with the position (42.235°) of the most intense peak of Fe_3W_3C phase (JCPDS card no. 41-1351). The presence of the brittle η-phase in X-6 hard metal has to be ascribed to sample decarburization during sintering and was responsible for the low TRS value (1326 MPa).

The position and the relative intensities of the two peaks at $2\theta = 43.7°$ and 50.8° confirmed the fcc-structure of the binder phase in the sintered samples [12]. The XRD spectra of WC–9 wt.% Fe/Ni/Co hard metals showed only peaks attributable to the fcc-binder phase and to WC. No η-phases were detected.

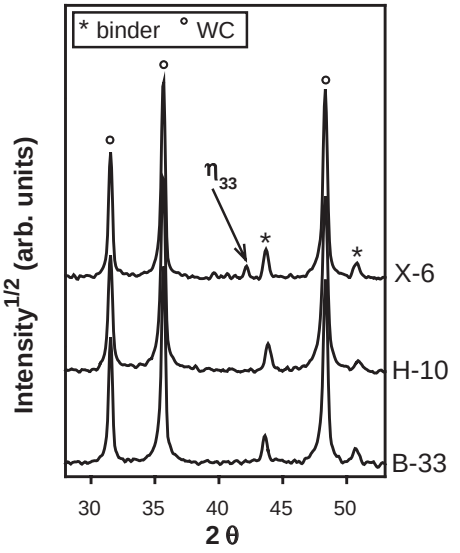

Fig. 2. XRD spectra (Cu Kα radiation) of hard metals sintered at 1500 °C. with 5.8 wt.% Fe/Ni/Co.

3.2. Pretreatments of Fe/Ni/Co–WC substrates

Cemented carbides contain Co, Ni or other transition metals acting as a binder and providing additional toughness to the sintered part. However, the presence of such transition metals is hostile to diamond adhesion [16–18]. The phase diagram of the Co–C system [27] predicts that, at the deposition temperatures of diamond (700–1000°C), carbon is soluble in Co up to 0.2–0.3 wt.%. During the initial stages of the CVD process, the WC–Co is exposed to a hydrocarbon radical-rich atmosphere and carbon species can rapidly diffuse into the bulk of the binder phase until the carbon solubility is exceeded. Cobalt, like Ni and Fe, is a transition metal with partially filled 3d shell, and it acts as a catalyst for the formation of graphite [16]. Therefore, once the carbon concentration at the substrate surface is sufficiently large for solid carbon condensation, the preferential formation of a graphite layer is promoted by the presence of the binder. The formation of a sp^2-carbon layer at the substrate surface during the early stages of deposition, on which scarcely adherent diamond grows later, has been shown as detrimental by several papers published in the relevant literature [19,28–30].

As a further consequence of C solubility into the binder phase, diffusion of carbon from the deposited diamond phase into the metal binder may occur at the high temperatures present in typical CVD growth conditions [31]. Voids form with time at the diamond/substrate interface, thus reducing the interfacial contact area and the adhesion strength. As a consequence, it is not possible to deposit adherent diamond coatings onto untreated cemented tungsten carbides and the binder phase must be removed from the substrate surface. A further issue that affects the adhesion of CVD diamond films to WC–Co substrates is the mechanical interlocking that occurs at the coating-carbide interface. In particular, recalling that adhesive toughness is a measure of the energy required to drive a crack along the interface between the film and the substrate, a rough interfacial microstructure would represent an obstacle to crack propagation, thus increasing adhesion [32]. Even in the presence of inter-nucleic voids, the presence of a rough interface might force the extending crack to follow a tortuous path, by deflecting it towards the bulk of the film and/or the substrate. Extension of the crack into the film or into the substrate may therefore pin the crack and thus arrest the interfacial crack [33].

Peters and Cummings [34] first introduced a two-step wet etching procedure, and which was effective in enhancing the adhesion of CVD diamond on WC–Co [35]. The first step uses a treatment with Murakami's reagent ($K_3[Fe(CN)_6]$/KOH/H_2O=1:1:10) to attack the WC grains, thus leading to substrate surface roughening. Afterwards, a H_2O_2–H_2SO_4 solution (Caro's acid) oxidizes the binder to soluble Co^{2+} compounds, thus reducing the surface Co concentration. In the case of WC–6 wt.% Co substrates, previous work showed that etching times as short as 5 s were sufficient to reduce the surface concentration of Co to a level which was below the detection limit of the EDS technique [8].

In an attempt to pretreat Fe/Ni/Co–WC substrates using the above-mentioned two-step chemical etching procedure, we noted that the second etching step with Caro's acid did not cause the surface binder removal, even for prolonged etching times. Fig. 3 shows that the Fe/Ni/Co binder alloy was still present at the surface of the H-10C substrate after 10 min etching with the H_2O_2–H_2SO_4 solution. Therefore, it was decided to study the kinetics of surface binder removal as a function of both the etching time and the etchant solution.

Fig. 4 shows the sum of Fe, Ni and Co concentrations measured by quantitative EDS analysis at the substrate surface of H-10C and H-15C cemented carbides as a function of the etching time. The data at time t=0 correspond to the EDS binder concentrations after WC etching with Murakami's solution, which led to surface binder enrichment. The results clearly showed that both diluted nitric acid and Caro's acid could not effectively remove the Fe/Ni/Co alloy from the hard metal surface, even after 10 min etching. As a matter of fact, the surface concentration of the binder alloy after 5 min etching with HNO_3/H_2O=1:1 or H_2O_2–H_2SO_4 was even larger than the binder bulk concentration (5.8 wt.%).

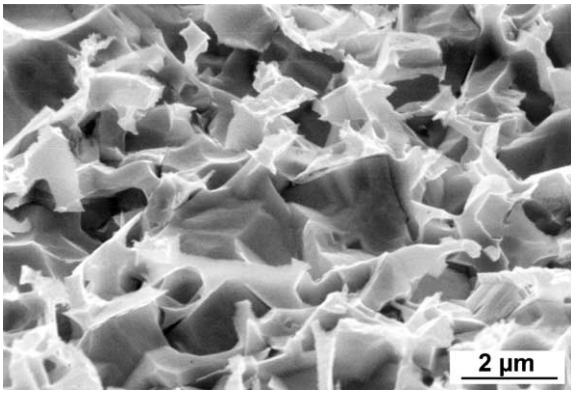

Fig. 3. SEM micrograph showing the surface of the H-10C hard metal after 10 min etching with Caro's acid (H_2O_2–H_2SO_4). The brighter Fe/Ni/Co alloy is clearly visible at the substrate surface.

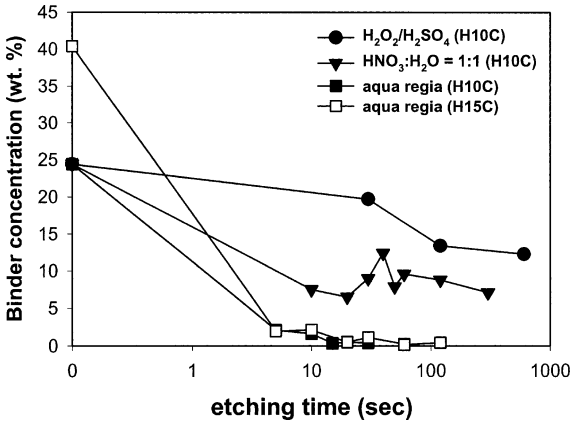

Fig. 4. Binder concentration (Fe+Ni+Co) at the substrate surface of H-10C (solid symbols) and of H-15C (open squares) Fe/Ni/Co-cemented carbide detected by EDS as a function of etching time and for different etchant solutions (T=30 °C). The data at time t=0 correspond to the alloy concentration after etching with Murakami's solution.

In contrast, aqua regia could reduce the surface concentration of the binder alloy to levels comparable to the EDS detection limit after just 20 s etching time. The depth of etching, i.e., the thickness of the binder-depleted layer after 20 s etching was uniform and around 5 μm, as assessed by SEM observation of the transverse section of etched samples (Fig. 5).

The low rates of surface binder removal observed when oxidizing etchants such as HNO_3/H_2O=1:1 or H_2O_2–H_2SO_4 were employed, confirmed the considerable improved corrosion and oxidation resistance of Co-containing binders with fcc-structures [12]. Therefore, the use of an exceptionally strong oxidizing agent such as aqua regia was necessary to achieve a fast binder removal from the substrate surface. Fig. 6 shows the typical hard metal surface morphology after the two-step etching procedure (Murakami's reagent and aqua regia).

3.3. Diamond film deposition and adhesion

On the basis of the results discussed in Section 3.1, it was decided to submit to diamond deposition only H-10C Fe/Ni/

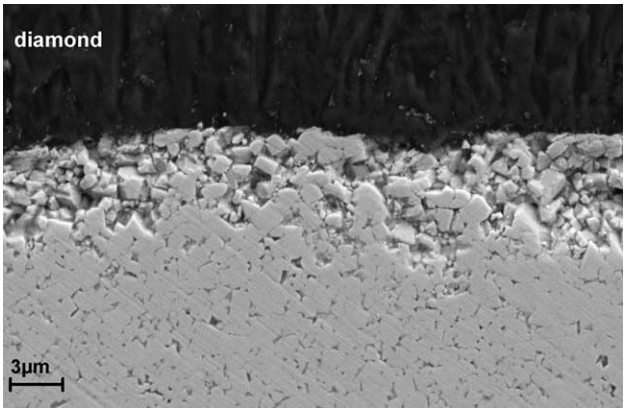

Fig. 5. Cross section of H-10C substrate after the two-step wet etching (10 min Murakami's reagent and 20 s aqua regia) and diamond deposition. The binder depleted region is about 5 μm thick.

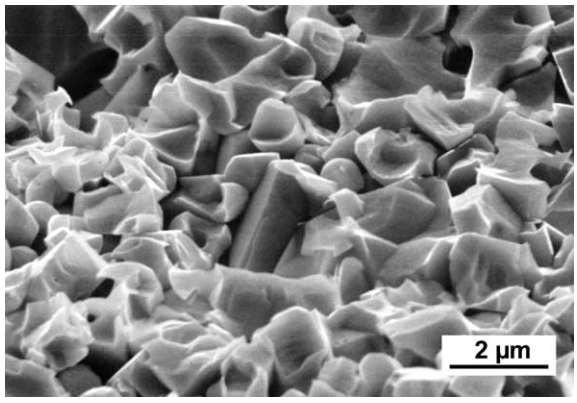

Fig. 6. Surface morphology of an H-15C substrate after two-step etching (10 min Murakami's reagent and 60 s aqua regia).

Co-cemented carbides, due to their larger toughness and hardness values. For the sake of comparison, we put in the HFCVD reactor also conventional H-4 WC–Co substrates with a microstructure comparable to that of H-10C samples sintered at the same temperature. Several samples for each hard metal grade were simultaneously deposited using the CVD conditions described in Section 2.2. Prior to deposition, WC–Co substrates were pretreated with Murakami's reagent for 10 min, rinsed with deionized water, etched with Caro's acid for 10 s and rinsed again with water. WC–Fe/Ni/Co substrates underwent a similar pretreatment, but we used aqua regia (20 s) to wash the surface binder out, as described in the previous paragraph.

The Raman spectra of the diamond films grown in the same deposition run on pretreated H-10C (WC–Fe/Ni/Co) and H4 (WC–Co) hard metal substrates are shown in Fig. 7. All samples exhibited similar spectra with an intense diamond peak at 1337 cm^{-1} and very weak sp^2-carbon bands in the 1450–

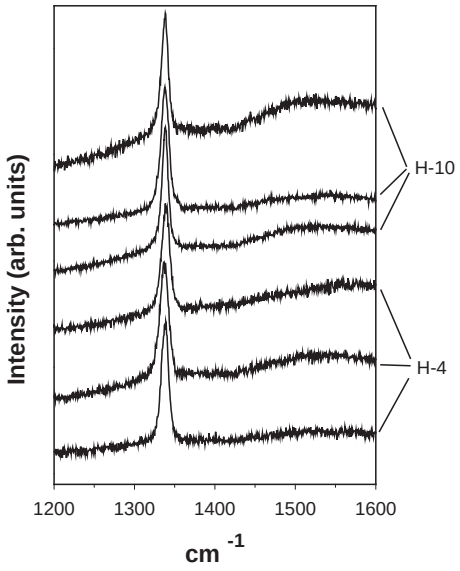

Fig. 7. Raman spectra of diamond films grown on WC–5.8 wt.% Fe/Ni/Co (H-10C) and WC–5.8 wt.% Co (H-4) substrates submitted to the same deposition run.

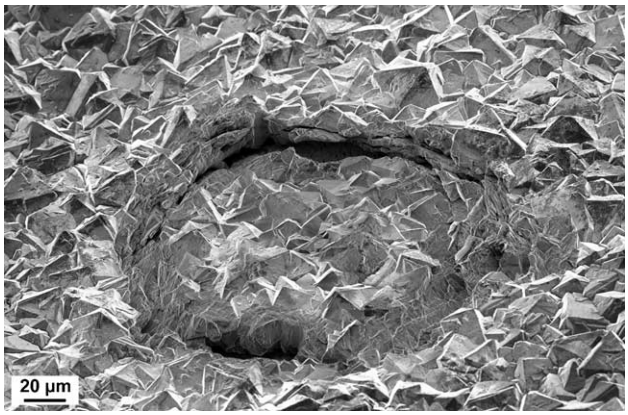

Fig. 8. Rockwell indentation test (60 kg) conducted on diamond film on H-15C substrate that has been surface modified by two-step wet chemical etching (Murakami's reagent and aqua regia).

1600 cm^{-1} range. This occurrence indicated that (i) all samples exhibited a large phase purity, independently of the binder nature, and (ii) the residual compressive stress of diamond was around 1.8 GPa [36].

In order to assess the adhesion level of diamond films onto WC–Fe/Ni/Co substrates and to compare their adhesion to those of diamond coatings grown on WC–Co substrates with the same binder phase content (6 wt.%), we performed indentation tests according to the procedure described in Section 2.3. Qualitatively, for films of equal thickness, the minimum load at which the coating fracture occurs (P_{cr}) by indentation can be used as a relative measure of adhesion. When fracture occurs, a lateral crack is initiated and propagated along the substrate–film interface, leading to debonding of the coating. The diamond films on H-10C substrates (medium-grained WC–6 wt.% Fe/Ni/Co) did not exhibit any sign of visible delamination for indentation loads of up to 60 kg (Fig. 8). The same results were observed for H-4 substrates (medium-grained WC–6 wt.% Co), thus confirming the effectiveness of the two-step etching procedure here employed to achieve good adherence of the films grown on WC–Fe/Ni/Co substrates.

4. Conclusions

Good-quality, dense cemented carbides with new binder phase were obtained by sinter-HIP of medium-grained WC and pre-alloyed Fe/Ni/Co powders. These new hard metals exhibited good mechanical properties, with hardness and toughness values close to those of conventional Co-cemented tungsten carbides having the same microstructure. Adherent diamond films were obtained on WC–6 wt.%Fe/Ni/Co substrates pretreated according to a modified Murakami two-step chemical etching. In fact, after the first etching step with Murakami's reagent, the use of aqua regia instead of Caro's acid was necessary to wash the surface binder phase out and to reduce its concentration to levels below the EDS detection limit. Surface roughening and surface binder removal allowed us to obtain good adherence of the films on WC–Fe/Ni/Co substrates, as quantified by Rockwell indentation tests.

These results showed that wear parts coated with CVD diamond can be obtained by a proper selection of WC–Fe/Ni/Co hard metal microstructure and of suitable pretreatments of the substrate surface prior to CVD.

Acknowledgments

The authors thank Dr. Giorgio Mattei (ISC-CNR) for Raman spectra and Mr. Giuseppe Piciacchia (ISC-CNR) for valuable technical collaboration. This work was partly funded by MIUR (Italian Ministry of Education, University and Research), whose financial support is gratefully acknowledged.

References

[1] Y.-W. Chung, W.D. Sproul, MRS Bull. 28 (3) (2003) 164.
[2] J.E. Field, The Properties of Diamond, Academic Press, London, 1979.
[3] Z.M. Zhang, H.S. Shen, F.H. Sun, X.C. He, Y.Z. Wan, Diamond Relat. Mater. 10 (2001) 33.
[4] S. Amirhaghi, H.S. Reehal, R.J.K. Wood, D.W. Wheeler, Surf. Coat. Technol. 135 (2001) 126.
[5] Y. Xie, R.J. Llewellyn, D. Stiles, Wear 250 (2001) 88.
[6] P. Niedzielski, S. Miklaszewski, P. Beer, A. Sokolowska, Diamond Relat. Mater. 10 (2001) 1.
[7] M.S. Raghuveer, S.N. Yoganand, K. Jagannadham, R.L. Lemaster, J. Bailey, Wear 253 (2002) 1194.
[8] R. Polini, F. Casadei, P. D'Antonio, E. Traversa, Surf. Coat. Technol. 166 (2003) 127.
[9] W. Ahmed, H. Sein, N. Ali, J. Gracio, R. Woodwards, Diamond Relat. Mater. 12 (2003) 1300.
[10] H. Sein, W. Ahmed, M. Jackson, R. Woodwards, R. Polini, Thin Solid Films 447–448 (2004) 455.
[11] T.S. Sudarshan, Met. Powder Rep. 53 (1998) 32.
[12] G. Gille, J. Bredthauer, B. Gries, B. Mende, W. Heinrich, Int. J. Refract. Met. Hard Mater. 18 (2000) 87.
[13] I.E. Clark, B.J. Kamphuis, Diamond Tooling Proceedings of Euro PM 2002 Lausanne, Switzerland, European Powder Metallurgy Association (EPMA), Shrewsbury, UK, 2002, p. 35.
[14] L. Prakash, Proceedings of 12th International Plansee Seminar, Reutte, vol. 2, 1993, p. 80.
[15] B. Wittmann, W.-D. Schubert, B. Lux, Hard Materials Proceedings of Euro PM 2002 Lausanne, Switzerland), European Powder Metallurgy Association (EPMA), Shrewsbury, UK, 2002, p. 303.
[16] X. Chen, J. Narayan, J. Appl. Phys. 74 (1993) 4168.
[17] M. Kawarada, K. Kurihara, K. Sasaki, Diamond Relat. Mater. 2 (1993) 1083.
[18] J. Narayan, M. Nelson, S. Oktyabrsky, K. Jagannadham, Mater. Sci. Eng., B, Solid-State Mater. Adv. Technol. 38 (1996) 46.
[19] F.-M. Pan, J.-L. Chen, T. Chou, T.-S. Lin, L. Chang, J. Vac. Sci. Technol., A, Vac. Surf. Films 12 (1994) 1519.
[20] P. XiLing, G. ZhaoPing, Thin Solid Films 239 (1994) 47.
[21] W. Zhu, R.C. McCune, J.E. deVries, M.A. Tamor, K.Y. Simon Ng, Diamond Relat. Mater. 3 (1994) 1270.
[22] S. Kubelka, R. Haubner, B. Lux, R. Steiner, G. Stingeder, M. Grasserbauer, Diamond Relat. Mater. 3 (1994) 1360.
[23] E.J. Oles, A. Inspektor, C.E. Bauer, Diamond Relat. Mater. 5 (1996) 617.
[24] I. Endler, A. Leonhardt, H.-J. Scheibe, R. Born, Diamond Relat. Mater. 5 (1996) 299.
[25] R.K. Singh, D.R. Gilbert, J. Fitz-Gerald, S. Harkness, D.G. Lee, Science 272 (1996) 396.
[26] P.C. Jindal, D.T. Quinto, G.J. Wolfe, Thin Solid Films 154 (1987) 361.
[27] H. Baker (Ed.), ASM Handbook, vol. 3, Alloy Phase Diagrams, ASM International, Metals Park, OH, USA, 1997.

[28] K. Shibuki, M. Yagi, K. Saijo, S. Takatsu, Surf. Coat. Technol. 36 (1988) 295.
[29] T.H. Huang, C.T. Kuo, C.S. Chang, C.T. Kao, H.Y. Wen, Diamond Relat. Mater. 1 (1992) 594.
[30] A. Inspektor, C.E. Bauer, E.J. Oles, Surf. Coat. Technol. 68/69 (1994) 359.
[31] A. Bock, W.D. Schubert, B. Lux, Powder Metall. Int. 24 (1992) 20.
[32] S. Kamiya, H. Takahashi, P. D'Antonio, R. Polini, E. Traversa, Diamond Relat. Mater. 11 (2002) 716.
[33] M.A. Taher, W.F. Schmidt, A.P. Malshe, E.J. Oles, A. Inspektor, K.L. Mittal (Ed.), Adhesion Aspects of Thin Films, vol. 1, VSP, The Netherlands, 2001, p. 79.
[34] M.G. Peters, R.H. Cummings, European Patent 0519587 A1 (1992).
[35] R. Haubner, A. Köpf, B. Lux, Diamond Relat. Mater. 11 (2002) 555.
[36] A. Tardieu, F. Cansell, J.P. Petitet, J. Appl. Phys. 68 (1990) 3243.